Friction compensation design based on state observer and adaptive law for high-accuracy positioning system*

WANG Ying, XIONG Zhenhua and DING Han**

(School of Mechanical Engineering, Shanghai Jiao Tong University, Shanghai 200030, China)

Received April 18, 2005; revised May 9, 2005

Abstract Friction is one of the main factors that affect the positioning accuracy of motion system. Friction compensation based on friction model is usually adopted to eliminate the nonlinear effect of friction. This paper presents a proportional-plus-derivative (PD) feedback controller with a friction compensator based on LuGre friction model. We also design a state observer to observe the unknown state of LuGre friction model, and adopt a parameter adaptive law and off-line approximation to estimate the parameters of LuGre friction model. Comparative experiments are carried out among our proposed controller, PD controller with friction compensation based on classical friction model, and PD controller without friction compensation. Experimental results demonstrate that our proposed controller can achieve better performance, especially higher positioning accuracy.

Keywords: friction compensation, state observer, adaptive law, linear motor, motion control.

Friction almost exists in any mechanical systems such as gear, valve, clutch, detent, and so on. In motion control applications, due to its high nonlinearity and complex characteristics, friction can affect the system's performance greatly. Friction often causes problems such as large steady-state error and limit cycle. For a motion system driven by rotary motors, there are some mechanical transmissions, which can reduce the effect of uncertainties and disturbances, like friction. However, for high accuracy positioning systems driven by linear motors, which are used more and more widely today[1,2], the effect of friction can be even worse. Therefore, when designing a controller for a directly driven system with the requirement of high positioning accuracy, we must reduce the effect of friction as low as possible.

Usually, friction compensation based on friction model is the basic method for eliminating friction and is used most widely. Since the 20th century, with more comprehension about friction phenomenon, many kinds of friction models have been proposed, such as the classical model, Karnopp model[3], Armstrong model[4], Dahl model[5], Bristle model[6] and LuGre model[7], etc. According to the descriptions of the behaviors of friction, these models can be divided into two kinds: static model and dynamic model. The former describes mainly the static behaviors of friction, including static friction, coulomb friction, viscosity friction, Stribeck effects, etc. While the latter describes not only the static behaviors of friction, but also the dynamic characteristics of friction, such as varying break-away force, frictional lag, stick-slip motion, and so on[8]. Among the models mentioned above, the first three models belong to the static model and the other three models are dynamic model.

Although many friction models have been presented by far, classical model is used most widely, since it is simple and easy to apply[9,10]. The classical model can be expressed as[11]:

$$\boldsymbol{F}_f = [\boldsymbol{F}_C + (\boldsymbol{F}_V - \boldsymbol{F}_C)e^{-(\dot{x}/\dot{x}_s)^{\delta}}]\mathrm{sgn}(\dot{\boldsymbol{x}}) + \boldsymbol{F}_V\dot{\boldsymbol{x}}, \quad (1)$$

where $\boldsymbol{F}_f$, $\boldsymbol{F}_C$, $\boldsymbol{F}_V$ represent static friction, coulomb friction, and viscosity coefficient, respectively; $\dot{\boldsymbol{x}}_s$ is the Stribeck velocity; $\dot{\boldsymbol{x}}$ is the velocity and δ is one experience value.

Although there are many successful applications of the classical model, the classical model is a static model. Thus, it cannot describe the dynamic behaviors of friction. However, these dynamic characteristics will affect the system's performance severely, especially for tracking performance and positioning accuracy. Therefore, when a motion system has higher

* Supported by National Natural Science Foundation of China (Grant No. 50390063), and the Science & Technology Commission of Shanghai Municipality (Grant Nos. 03XD14008 and 041111006)

** To whom correspondence should be addressed. E-mail: hding@sjtu.edu.cn

requirements for positioning accuracy, friction compensation based on the classical model is difficult to satisfy the performance requirements.

Among the dynamic models, LuGre model has received more and more attentions these years[12—14], since it describes the behaviors of friction more completely and concisely. However, LuGre model has quite many parameters and an unknown state, which makes its realization much difficult and complicated. So, LuGre model is seldom applied.

In this paper, friction compensation is realized based on LuGre model. We design a state observer to observe the unknown states and adopt a parameter adaptive law and off-line approximation to estimate the parameters of LuGre model. Thus, we give an easy way to realize the friction compensation based on LuGre model. In the experiments, we will also compare the controller with the other two controllers. Experimental results show that our proposed controller can achieve lower tracking error and higher positioning accuracy.

1 Motion control system

Figure 1 depicts an experimental motion control system in the Advanced Electronic Manufacturing Center of SJTU. This system is an X-Y table driven by permanent-magnet iron-coreless linear motors. The table has a work area of about 150 mm × 150 mm. The linear encoder resolution is 0.5 μm. The motors are PLATINUM DDL series motors from Kollmorgen™. This system is an experimental prototype of high-performance positioning systems, which are used in various phases of microelectronic manufacturing such as wire bonding and die mounting.

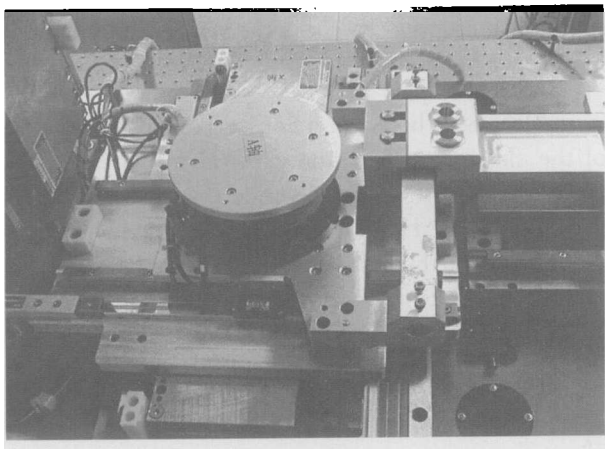

Fig. 1. The motion control platform.

Fundamentally, a linear motor is a rotary motor when it is rolled out flat, so the working principle of the linear motor is nearly the same as the rotary motor. Hence, the dynamics of one axis of the motor system can be expressed simply as

$$\boldsymbol{u} - \boldsymbol{F}_{\mathrm{f}} = M\ddot{\boldsymbol{x}}, \tag{2}$$

where $\boldsymbol{u}$ denotes control force; $\boldsymbol{F}_{\mathrm{f}}$ is the friction; M is the inertia of the table and $\boldsymbol{x}$ is the displacement of the table.

Generally, there are many nonlinear factors and uncertainties in systems driven by linear motors. Among them, force ripple is one major factor affecting the system's performance. Force ripple usually comes from cogging force and magnetic reluctance force. Since the linear motors in our control system are iron-coreless motors, force ripple is small. Therefore, in this model, we just consider the effect of friction and ignore the effect of force ripple.

2 Friction compensation

2.1 LuGre model

Canudas et al.[7] thought that two rigid bodies contacted through elastic bristles. When a tangential force was applied, the bristles would deflect like springs, which gave rise to the friction force. They proposed a new dynamic model for friction as follows:

$$\frac{\mathrm{d}\boldsymbol{z}}{\mathrm{d}t} = \boldsymbol{v} - \frac{|\boldsymbol{v}|}{g(\boldsymbol{v})}\boldsymbol{z}, \tag{3}$$

$$\sigma_0 g(\boldsymbol{v}) = \boldsymbol{F}_{\mathrm{C}} + (\boldsymbol{F}_{\mathrm{S}} - \boldsymbol{F}_{\mathrm{C}})\mathrm{e}^{-(\boldsymbol{v}/\boldsymbol{v}_{\mathrm{s}})^2}, \tag{4}$$

$$\boldsymbol{F}_{\mathrm{f}} = \sigma_0 \boldsymbol{z} + \sigma_1 \frac{\mathrm{d}\boldsymbol{z}}{\mathrm{d}t} + \sigma_2 \boldsymbol{v}. \tag{5}$$

where $\boldsymbol{v}$ is the relative velocity between the two surfaces; $\boldsymbol{z}$ denotes the average deflection of the bristles; σ_0, σ_1, σ_2 denote stiffness damping coefficient and viscous coefficient, respectively; $\boldsymbol{F}_{\mathrm{C}}$ is Coulomb friction; $\boldsymbol{F}_{\mathrm{S}}$ is static friction; and $\boldsymbol{v}_{\mathrm{s}}$ is Stribeck velocity. Furthermore, Canudas et al. suppose that $g(\boldsymbol{v})$ is always strictly positive real and is bounded.

2.2 Controller design

LuGre model has an unknown and immeasurable state variable $\boldsymbol{z}$, which makes the realization difficult. In order to overcome this difficulty, a state observer is designed in this paper to observe $\boldsymbol{z}$. The observer is

$$\dot{\hat{\boldsymbol{z}}} = \dot{\boldsymbol{x}} - \phi(\dot{\boldsymbol{x}})|\dot{\boldsymbol{x}}|\hat{\boldsymbol{z}} - k\phi(\dot{\boldsymbol{x}})|\dot{\boldsymbol{x}}|\boldsymbol{r} + \frac{k\sigma_0}{\sigma_1}\boldsymbol{r}, \tag{6}$$

where $\phi(\dot{x}) = 1/g(\dot{x})$, $r = \dot{e} + \lambda e$, $e = x_d - x$. x_d is the desired reference displacement, and λ, k are positive coefficients. Since $g(\dot{x})$ is always strictly positive real and is bounded, we assume $\phi(\dot{x}) \leqslant \beta$ without loss of generality, where β is a positive constant.

We also adopt an adaptive law given below to estimate the viscosity coefficient σ_2:

$$\dot{\hat{\sigma}}_2 = k_2 \dot{x} r, \tag{7}$$

where k_2 denotes a positive adaptive gain.

Then from Eq. (5), friction can be estimated by

$$\hat{F}_f = \sigma_0 \hat{z} + \sigma_1 \dot{\hat{z}} + \hat{\sigma}_2 \dot{x}. \tag{8}$$

Now a controller with the friction estimation is

$$u = M\ddot{x}_d + K_D r + \hat{F}_f + k\sigma_1 \beta |\dot{x}| r, \tag{9}$$

where K_D is positive.

Since $r = \dot{e} + \lambda e$, the right second term of Eq. (9) actually is a PD controller, whose proportional gain K_P is $K_D\lambda$, and the derivative coefficient is K_D.

To ensure the stability of the system, we can choose a function

$$V = \frac{1}{2}Mr^2 + \frac{\lambda}{2}(2K_D - M\lambda)e^2 + \frac{\sigma_1}{2k}\tilde{z}^2 + \frac{1}{2k_2}\tilde{\sigma}_2^2, \tag{10}$$

where $\tilde{z} = \hat{z} - z$, $\tilde{\sigma}_2 = \hat{\sigma}_2 - \sigma_2$.

Its derivative is

$$\dot{V} = Mr\dot{r} + \lambda(2K_D - M\lambda)e\dot{e} + \frac{\sigma_1}{k}\tilde{z}\dot{\tilde{z}} + \frac{1}{k_2}\tilde{\sigma}_2\dot{\tilde{\sigma}}_2. \tag{11}$$

Substituting Eqs. (2)—(9) into Eq. (11), we have

$$\begin{aligned} V &= Mr\dot{r} + \lambda(2K_D - M\lambda)e\dot{e} \\ &\quad - \frac{\sigma_1}{k}\phi(\dot{x})|\dot{x}|\tilde{z}^2 - \sigma_1\phi(\dot{x})|\dot{x}|\tilde{z}r \\ &\quad + \sigma_0\tilde{z}r + \tilde{\sigma}_2\dot{x}r \\ &= Mr\dot{r} + \lambda(2K_D - M\lambda)e\dot{e} - M\ddot{e}r - K_D r^2 \\ &\quad - \sigma_0 k r^2 - k\sigma_1\beta|\dot{x}|r^2 + k\sigma_1\phi(\dot{x})|\dot{x}|r^2 \\ &\quad - \frac{\sigma_1}{k}\phi(\dot{x})|\dot{x}|\tilde{z}^2. \end{aligned} \tag{12}$$

Since $0 < \phi(\dot{x}) \leqslant \beta$, Eq. (12) can be further simplified as

$$\begin{aligned} \dot{V} &\leqslant M\lambda r\dot{e} + \lambda(2K_D - M\lambda)e\dot{e} - K_D r^2 \\ &= M\lambda\dot{e}^2 + 2\lambda K_D e\dot{e} - K_D\dot{e}^2 - 2K_D\lambda e\dot{e} - K_D\lambda^2 e^2) \\ &= -K_D\lambda^2 e^2 - (K_D - M\lambda)\dot{e}^2. \end{aligned} \tag{13}$$

In Eq. (13), if parameter K_D and λ satisfy $K_D \geqslant M\lambda$, then $V > 0$ and $\dot{V} \leqslant 0$. Based on Lyapunov's stability theory, the system is globally stable. Furthermore, by applying LaSalle and Barbalat theorem, e and $\dot{e}$ are asymptotically convergent to zero.

2.3 LuGre model parameter estimation

The LuGre model given by Eqs. (3), (4) and (5) is characterized by six parameters, σ_0, σ_1, σ_2, F_C, F_S and v_s. Among them, F_C, F_S, σ_2 and v_s can be determined by measuring the steady-state friction force when the velocity is held constant. For steady-state motion, $dz/dt = 0$, from Eq. (3) we have

$$z_{ss} = \frac{v}{|v|}g(v) = g(v)\mathrm{sgn}(v). \tag{14}$$

Substituting Eq. (14) into Eqs. (4) and (5), the friction force in steady-state motion is given by

$$\begin{aligned} F_{SS}(v) &= \sigma_0 g(v)\mathrm{sgn}(v) + \sigma_2 v \\ &= [F_C + (F_S - F_C)e^{-(v/v_s)^2}]\mathrm{sgn}(v) \\ &\quad + \sigma_2 v. \end{aligned} \tag{15}$$

On the other hand, from Eq. (2), when the velocity is constant, we have

$$F_{SS}(v) = u. \tag{16}$$

Note that if the input u is held constant, the velocity reaches the steady state. When this happens, Eq. (16) must be satisfied. By repeating such experiments for various inputs u, a relation between friction force and velocity can be obtained. Then, by Eq. (15), F_C, F_S, σ_2 and v_s can be estimated.

In addition, Eq. (15) shows that for steady-state motion LuGre model is just the same as the classical model. However, compared with the classical model, LuGre model describes friction more completely, because besides the characteristics considered by the classical model, LuGre model still considers an important state variable, i.e. tiny displacement.

The other two parameters, σ_0 and σ_1, can be estimated by the method described as follows: When the motion system receives an external force and it does not move visibly, the following assumptions can be made: $z \approx x$ and $dz/dt \approx v$.

Thus, Eq. (5) can be appropriated by

$$F_f \approx \sigma_0 x + \sigma_1 \dot{x} + \sigma_2 \dot{x}, \quad (17)$$

and the model of the motion system can be represented by

$$M\ddot{x} + (\sigma_1 + \sigma_2)\dot{x} + \sigma_0 x = u. \quad (18)$$

By using Laplace transform, Eq. (18) is rewritten as

$$\frac{x(s)}{u(s)} = \frac{1}{Ms^2 + (\sigma_1 + \sigma_2)s + \sigma_0}. \quad (19)$$

Eq. (19) shows that when the motion system receives an external force and it does not move visibly, the system behaves like a damped second order system. Thus σ_0 and σ_1 can be estimated by matching its step input response.

3 Experimental results

3.1 Estimate the parameters of friction model

In the first step, we will estimate the parameters F_C, F_S, σ_2 and v_s. Figure 2 shows the relation between the input current and the velocity obtained from experiments. We only give the relation in the positive direction. The relation in the negative direction is similar. In addition, since friction force varies during the motions, the measured data are average values.

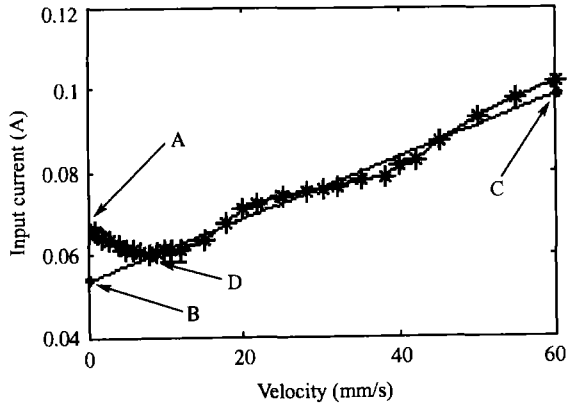

Fig. 2. Experimental curve of velocity versus current.

According to Fig. 2, the friction force model can be obtained by multiplying a proportional factor K_f. Points A and B correspond to the static friction F_S and the Coulomb friction F_C, respectively. Line "BC" approximates the increasing experimental curve. Its slope corresponds to the viscous coefficient. The Stribeck velocity v_s can be determined by approximating the decreasing experimental curve "AD". All the approximations adopt least squares method, i.e. the sum of squares of errors between the actual measurement data and the fitting curve is the least.

In the second step, we will estimate parameters σ_0 and σ_1. By using the software for linear motor from Servostar MotionLink™, we can have an online open-loop test. Figure 3 shows the response of the motion system to a 0.036 amperes step input. In Fig. 3, some indexes of step input response can be calculated, such as overshoot, steady-state error, and so on. Then according to Eq. (17), σ_0 and σ_1 can be obtained.

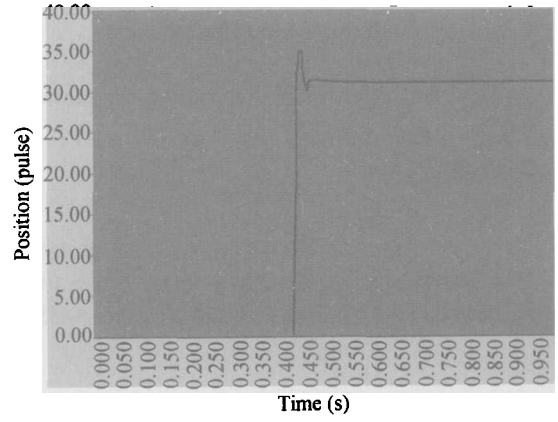

Fig. 3. Position response to 0.036 A step input. (2000 pulses are equal to 1 millimeter.)

The estimated parameters of the friction model are shown in Table 1.

Table 1. Estimated parameter values

F_C (N)	F_S (N)	v_s (m/s)	σ_0 (Ns/m)	σ_1 (Ns/m)	σ_2 (Ns/m)
9.08	11.20	0.0045	19000.0	1663.2	136.8

3.2 Experimental results

Three different controllers were implemented for one axis motion (X axis) to compare their performance: the first controller is PD controller, the second one is PDFC (PD plus friction compensation based on classical model), and the third one is PDLA (our proposed controller, i.e. PD plus Friction compensation based on LuGre model with state observer and parameter adaptive law). The classical model is shown in Eq. (13), and its parameters are given in Table 1. In addition, PD controllers' parameters in the three controllers are the same for more proper and convictive comparative results.

It is known that, if a system works at several

different velocity and acceleration levels, its responses are quite different. Therefore, to better show the effect of friction compensation, we implement experiments in both cases of low speed low acceleration and high-speed high acceleration.

3.2.1 Low speed and low acceleration case

The desired trajectory is planned by the S-curve profile that is the most common motion planning profile. The target displacement is set to be 2 mm; the velocity is 0.5 mm/s; the acceleration is 0.2 m/s^2 and the jerk is 30 m/s^3. PD controller parameters are $K_D = 20$ and $K_P = K_D\lambda = 3$. The experimental results are shown in Fig. 4 and Fig. 5.

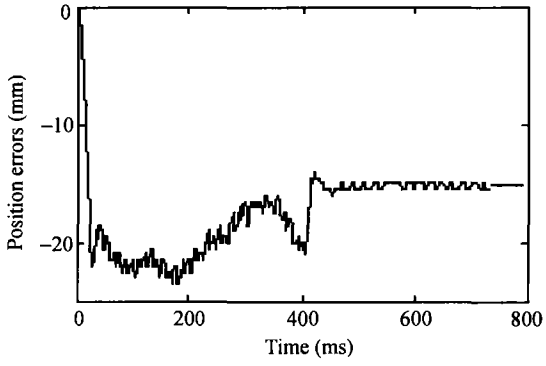

Fig. 4. Tracking errors of PD controller for low speed and low acceleration.

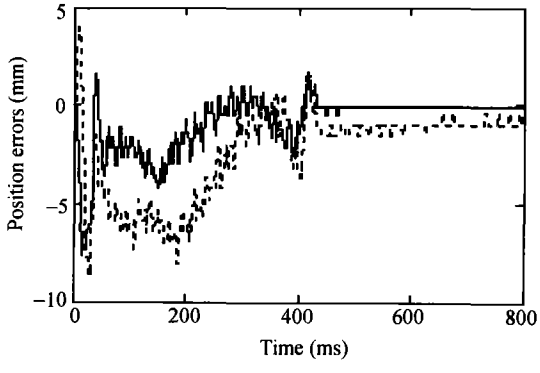

Fig. 5. Tracking errors for low speed and low acceleration (solid line: PDLA; dotted line: PDFC).

Figure 4 shows that the tracking error of the PD controller without any friction compensation is large, and the steady-state error is about 15 μm. Furthermore, there is limit cycle around the steady-state position. In Fig. 5, both PDFC and PDLA improve the dynamic and steady-state performance of PD. Between them, PDLA performs better than PDLA, as it not only reduces the steady-state error to about 1 μm, but also eliminates limit cycle.

3.2.2 High-speed and high acceleration case

The desired trajectory is also planned by S-curve profile. The target displacement is 8 mm; the velocity is 200 mm/s; the acceleration is 40 m/s^2 and the jerk is 3×10^4 m/s^3. PD controller parameters are $K_D = 25$, and $K_P = K_D\lambda = 0.5$. The experimental results are shown in Fig. 6 and Fig. 7.

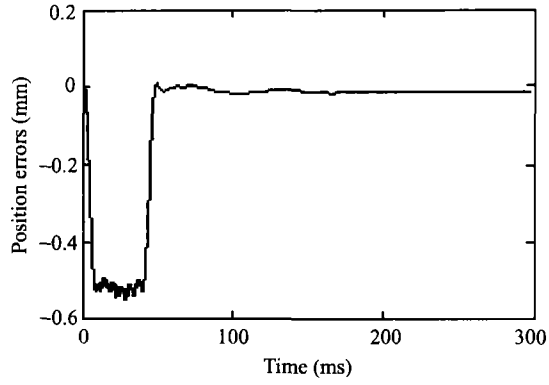

Fig. 6. Tracking errors of PD controller for high speed and high acceleration.

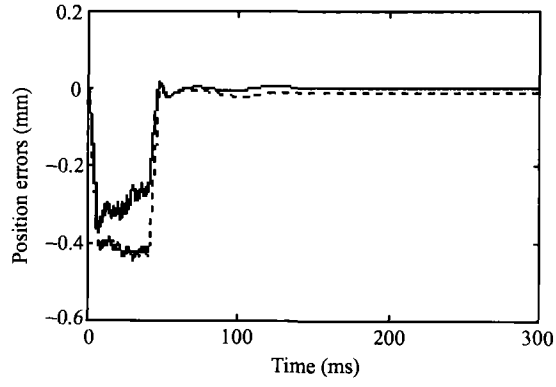

Fig. 7. Tracking errors for high speed and high acceleration (solid line: PDLA; dotted line: PDFC).

Evidently, the dynamic tracking error of the PD controller is the largest, and that of PDLA is the least. In order to show the steady-state errors of them clearly, Fig. 8 redraws the steady-state errors of the three controllers. It can be seen that the steady-state error of PD controller varies between ±4 μm around −15 μm, while that of PDFC varies between ±2.5 μm around −6 μm, and that of PDLA varies between ±1 μm around −1 μm.

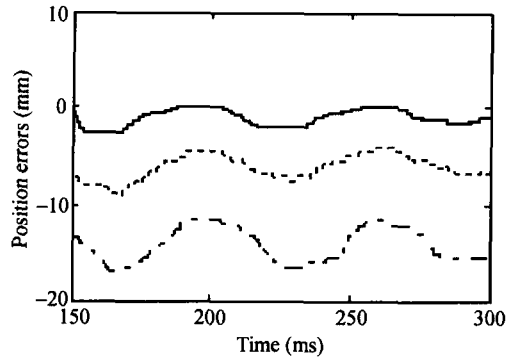

Fig. 8. Steady-state errors for high speed and high acceleration (solid line: PDLA; dotted line: PDFC; dashed line: PD).

3.3 Experimental results analysis

The experimental results show that both PDLA and PDFC can improve performance to some extent. However, PDLA can achieve much lower tracking error and higher positioning accuracy, which can be owed to two reasons: one is that LuGre model describes friction more accurately than the classic model, and especially it considers tiny displacement, which tends to raise the positioning accuracy. The other is that PDLA adopts the parameter adaptive law, which can reduce the errors of model parameters.

Although friction compensation can improve the system's dynamic and steady-state performances, when the speed and acceleration become higher, the system's dynamic performances get worse. The reason is that when the speed and the acceleration are low, friction is the main factor to affect the system's performance. Hence friction compensation can achieve good results. When the speed and acceleration are higher, besides friction, there are many other factors like the system's high frequency characteristics, uncertain nonlinearities and disturbances. Therefore, under this circumstance, sole friction compensation may not satisfy the performance requirements.

4 Conclusion

In this paper, a simple realization of friction compensation based on LuGre model has been presented by designing state observer and parameter adaptive law. Furthermore, we have compared the proposed controller (PDLA) with other two controllers, namely proportional-plus-derivative (PD) and PD plus friction compensation based on classical model (PDFC). Experimental results have demonstrated the effectiveness of our proposed controller.

We find that PDLA is simple to design, easy to realize, and able to achieve smaller tracking error and higher positioning accuracy. Although when speed and acceleration become higher, PDLA may not improve the performance as greatly as in the case of low speed and low acceleration, PDLA does improve the performance quite a bit. It still achieves high positioning accuracy of about 2 μm for high speed and high acceleration case. Therefore, our proposed controller is highly fit for the applications where high acceleration and high positioning accuracy are required, such as microelectronic packaging systems.

References

1 Tan K. K., Dou H. F. and Tang K. Z. Precision motion control system for ultra-precision semiconductor and electronic components manufacturing. In: Electronic Components and Technology Conference, Orlando, USA, May 29-Jun 1, 2001, 1372—1379.
2 Braembussche P. V., Swevers J., Brussel H. V. *et al*. Accurate tracking control of linear synchromous motor machine tool axes. Mechatronics, 1996, 6(5): 507—521.
3 Karnopp D. Computer simulation of slip-stick friction in mechanicaldynamic systems. Journal of Dynamic Systems, Measurement and Control, 1985, 107(1): 100—103.
4 Armstrong-Hélouvry B., Dupont P. and Canudas W. C. A survey of models, analysis tools and compensation methods for the control of machines with friction. Automatica, 1994, 30(7): 1083—1138.
5 Dahl P. Solid friction damping of spacecraft oscillations. In: Proc. AIAA *Guidance and Contr. Conf.*, Boston, USA, 1975, 75—1104.
6 Haessig D. A. and Friedland B. On the modeling and simulation of friction. J. Dyn. Syst. Meas. Control. Trans. ASME, 1991, 113(3): 354—362.
7 Canudas C., Olsson H., Astrom K. J. et al. A new model for control of systems with friction. IEEE Transactions on Automatic Control, 1995, 40(3): 419—425.
8 Chen H. and Pan Y. C. Dynamic behavior and modeling of the pre-sliding static friction. Wear, 2000, 242(1): 1—17.
9 Lee H. S. and Tomizuka M. Robust motion controller design for high-accuracy positiong systems. IEEE Transactions on Industrial Electronics, 1994, 43(1): 48—55.
10 Arkan K. J., Francis D. III. Friction compensation for a process control valve. Control Engineering Practice, 2000, 8 (7): 799—812.
11 Lee T. H., Tan K. K., Huang S. N. et al. Intelligent control of precision linear actuators. Engineering Applications of Artificial Intelligence, 2000, 13(6): 671—684.
12 Misovec K. M. and Annaswamy A. M. Friction compensation using adaptive nonlinear control with persistent excitation. In: Proceedings of the 1998 American Control Conference, Philadelphia, USA, June 24—26, 1998, 1483—1487.
13 Olsson H. and Astrom K. J. Observer-based friction compensation. In: Proceedings of the 35th Conference on Decision and Control, Koba, Japan, December 11—13, 1996, 4345—4350.
14 Laura R. R., Ashok R. and Jennifer T. Adaptive friction compensation using extended Kalman-Bucy filter friction estimation. Control Engineering Practice, 2001, 9(2): 169—179.